



Haptic rendering of sharp objects using lateral forces

Otniel Portillo-Rodríguez, Carlo Alberto Avizzano, Massimo Bergamasco,
Gabriel Robles-De-La-Torre

Abstract – Achieving realistic rendering of thin and spatially sharp objects (needles, for example) is an important open problem in computer haptics. Intrinsic mechanical properties of users, such as limb inertia, as well as mechanical and bandwidth limitations in haptic interfaces make this a very challenging problem. A successful rendering algorithm should also provide stable contact with a haptic virtual object. Here, perceptual illusions have been used to overcome some of these limitations to render objects with perceived sharp features. The feasibility of the approach was tested using a haptics-to-vision matching task. Results suggest that lateral-force-based illusory shapes can be used to render sharp objects, while also providing stable contact during virtual object exploration.

I. INTRODUCTION

AN important, open problem in computer haptics [1,2] is the force-feedback-based rendering of thin objects such as needles and, in general, of objects with spatially sharp physical features. During interaction with force-feedback virtual objects, important high-frequency spatial information about sharp features is lost due to mechanical and bandwidth limitations of force-feedback interfaces. This makes it challenging to produce adequate, stable haptic rendering of thin, sharp haptic objects.

It has been found that force-feedback information alone can elicit complex perceptions relating to haptic texture and shape [3-7]. Such perceptions can be considered as haptic perceptual illusions of texture and shape. This article explores the feasibility of using one of these perceptual phenomena to render haptic surfaces with spatially sharp surface features. In this article, lateral forces [5,6] have been used to design haptic surfaces with sharp, illusory bumps. A haptics-to-vision matching task has been used to assess human perception and performance during user exploration of these surfaces, as well as during the exploration of surfaces with real, sharp surface features.

The principal motivation of this work is creating a framework to exploit haptic illusions to modify user perception and help overcome physical limitations of haptic interfaces when rendering sharp objects. In this way it would be possible, for example: a) to render complex geometries, b) to allow manipulation of micro features, c) to improve the

stability of the contact with virtual objects.

II. METHODS

A. Experimental setup

Subjects interacted with the virtual surfaces and made judgments about them. They used a GRAB haptic interface [8-10] (Fig. 1) through a thimble-like attachment in which they inserted the index finger of their right hand. The GRAB interface allows users to touch 3D virtual surfaces with the index fingertip while moving their hand along a desktop workspace. As the user moves his/her finger over the virtual surface, he/she feels contact forces at the fingertip and can experience the virtual surface's geometric features (such as corners, surface edges, curvature, etc.), distinguish sizes and distances and understand spatial relationships between elements.



Fig 1. Experimental setup. Subjects explored the haptic virtual surfaces through a GRAB interface. A thimble-like manipulandum was used. During exploration, subjects listened to broadband noise to mask auditory cues. Subjects closed their eyes during whole exploration. After exploring the haptic surfaces, the profiles of four different surfaces (Fig. 3) were displayed on the computer monitor.

During the experiments, subjects' were instructed to maintain their finger inserted into the thimble at all times. By doing this, they avoided any kind of accidental contact with other parts of GRAB. At the beginning of a trial, the experimenter moved GRAB's thimble to the starting position at the right side of GRAB's workspace (Fig. 4). Subjects were instructed to explore the virtual surface by sliding their finger sideways (left-right) along the virtual surface. Subjects explored the virtual surface at their own pace. There was no time limit to explore the surface, but subjects were encouraged to proceed with some speed. Before they started exploring the surface, subjects closed their eyes. They kept them closed during the exploration. To

Manuscript received March 15, 2006. This work was supported in part by Enactive and Intuition European Excellence Networks.

Otniel Portillo-Rodríguez, Carlo Alberto Avizzano and Massimo Bergamasco are with Perceptual Robotics Laboratory (PERCRO), Scuola Superiore Sant'Anna, Pisa, Italy (phone: +39 050-883-071; fax: +39 050-883-333; e-mail: carlo@sssup.it).

Gabriel Robles-De-La-Torre is with the International Society for Haptics. (e-mail: Gabriel@RoblesDeLaTorre.com).

mask auditory cues to the interface's operation, subjects listened to broadband noise through headphones. Fig. 2 shows the architecture of the experimental setup.

During the experiment, a series of computer-generated haptic surfaces were presented to the subjects. The surfaces were not presented in any particular order. Each presentation of a surface defined a trial. The shape of the surface changed from trial to trial. Subjects experienced different qualities about the surfaces, such as their texture and shape. They were asked to concentrate on perceiving how the shape of the surface felt like.

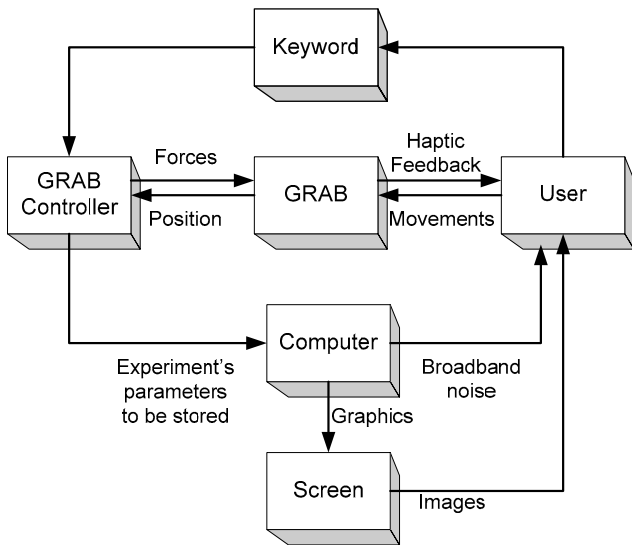


Fig 2. Experiment's Architecture.

When subjects finished haptically exploring each shape, they matched the haptic shape to a visually displayed profile. A set of shape profiles was visually shown to subjects on a computer screen (Fig. 3). Each profile had a number. Subjects used a computer keyboard to enter the number of the profile that they believed to be closest to the profile of the shape that was haptically explored. If they were not completely certain about the shape, subjects were instructed to give their best guess. The following variables were saved during the experiment: trajectory of GRAB's thimble during exploration, trial exploration time, haptic shape presented and visual shape matched. A test consisted of 90 trials, and typically lasted for 25 minutes.

B. Subjects

Ten right-handed subjects ages 21–37 participated in the experiment. All subjects had previous experience with haptic interfaces, but were naïve as to the purpose of the experiment. Subjects did not self-report any hand injury or disease. All subjects gave informed consent prior to testing. The experimentation was approved by PERCRO's review board. The participation was voluntary and the subjects had the right to withdraw their consent or discontinue participation at any time.

C. Haptic Surfaces

Five different haptic surfaces were used in this experiment: 1) a sinusoidal segment, 2) a sinusoidal segment with a lateral-force-based [5,6] illusory Gaussian shape, 3) a sawtooth segment, 4) a sinusoidal segment with a small sawtooth bump, and 5) a sinusoidal segment with a small Gaussian bump. The force-feedback and geometrical features of each surface are described below. A surface was rendered with lateral (along the x-axis, F_x , see Fig. 4) and vertical forces (along the y-axis, $y(x)$, see Fig. 4). The vertical forces were servoed to maintain the vertical position of the haptic manipulandum as close as possible to the target geometry of each surface. Vertical forces thus depended on the forces applied vertically by subjects during exploration. Lateral forces, however, did not depend on subjects' applied force, unlike previous experiments on the perceptual role of lateral forces [6]. However, it has been found that perception of haptic shape can be elicited through lateral forces that are independent of vertical force applied [5].

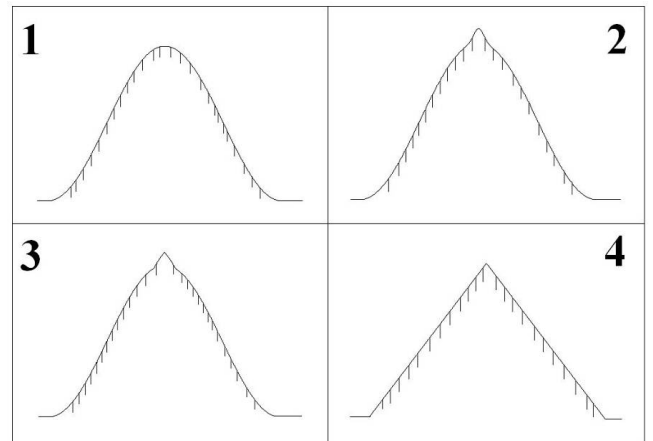


Fig. 3. Surface profiles that were visually displayed to subjects after exploring each haptic surface. Subjects chose the shape that best matched the haptically explored surface. Profile 1 was a sinusoidal segment. Profiles 2-4 showed different objects with sharp features. Profile 2 was a sinusoidal segment with a Gaussian-shaped bump. Profile 3 was a sinusoidal segment with a small, sawtooth bump. Profile 4 was a large sawtooth segment.

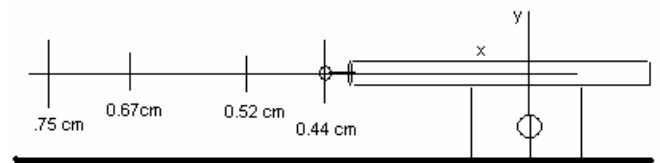


Fig. 4. Reference system of the GRAB.

The virtual surfaces were displayed within a 0.31m workspace along the interface's x-axis (Fig. 4). Two vertical virtual walls delimited the workspace. The virtual surfaces were centered at c , which was randomly varied from trial to trial from 0.52m to 0.67m. All sinusoidal segments were generated with a spatial period $T = 0.1$ m, and amplitude $A = 0.01$ m. All Gaussian shapes had a width $\omega = 0.003$ m. The haptic rendering was performed at 2.5 kHz.

The definition of the haptic shapes follows. This definition describes the force and geometrical features that defined the shapes, including the workspace location in which these features appeared. Outside of such workspace locations, a flat haptic surface was rendered as a default. In what follows, x is the position of the subject's fingertip along the x -axis.

C.1 Sinusoidal segment ("SineSeg", Fig. 5, case A).

The geometry of this shape was defined by:

$$y_1(x) = \frac{A}{2} \cos\left(\frac{2\pi}{T}(x-c)\right) + \frac{A}{2} \quad \forall x \in \left(c - \frac{T}{2}, c + \frac{T}{2}\right) \quad (1)$$

The lateral forces (x -force direction) were given by

$$F_{x1} = -\frac{A\pi}{T} \sin\left(\frac{2\pi}{T}(x-c)\right) \quad \forall x \in \left(c - \frac{T}{2}, c + \frac{T}{2}\right) \quad (2)$$

Otherwise $y_1(x) = F_{x1} = 0$.

C.2 Sinusoidal segment with lateral-force-based Gaussian surface ("SineLFGauss", Fig. 5, case B).

This shape consisted of SineSeg plus a lateral-force-based illusory Gaussian shape [5,6], which was positioned at the highest point of SineSeg. The geometry of SineLFGauss was the same as that of SineSeg (described above).

$$y_2(x) = y_1(x) \quad \forall x \in \left(c - \frac{T}{2}, c + \frac{T}{2}\right) \quad (3)$$

The lateral forces of this surface were also those of SineSeg plus the Gaussian component:

$$F_{x2} = F_{x1} + \frac{2k}{\omega^2} (x-c) e^{-\left(\frac{x-c}{\omega}\right)^2} \quad (4)$$

Otherwise, $y_2(x) = F_{x2} = 0$. A value of $k=0.01$ m was chosen based on previous experiments with this type of stimulus [5,6].

C.3 Sawtooth segment ("Saw", Fig. 5, case C).

The slope of the sawtooth is equal to the maximum slope of SineSeg, $m = \mp \frac{A\pi}{T}$, which occurs at $x = c \pm \frac{T}{4}$. With these parameters, the Sawtooth segment was defined by:

$$\begin{cases} \text{If } x < c \\ y_3(x) = \frac{A\pi}{T} \left(x - \left(c - \frac{T}{4}\right)\right) + \frac{A}{2} \\ F_{x3} = -\frac{A\pi}{T} \\ \forall x \in \left(c - \frac{T}{2}, c\right) \end{cases} \quad \begin{cases} \text{If } x \geq c \\ y_3(x) = -\frac{A\pi}{T} \left(x - \left(c + \frac{T}{4}\right)\right) + \frac{A}{2} \\ F_{x3} = \frac{A\pi}{T} \\ \forall x \in \left(c, c + \frac{T}{2}\right) \end{cases} \quad (5) \quad (6)$$

In both cases, if $y_3(x) \leq 0$ then $y_3(x) = F_{x3} = 0$.

C.4 Sinusoidal segment with small sawtooth bump ("SineSaw", Fig. 5, case D).

The sinusoidal component of this surface is also SineSeg. The small sawtooth bump has a slope equal to the greatest slope of SineGauss (below) which occurs at:

$x = c \pm \frac{\sqrt{2}}{2} |w|$ and its value are $m = \mp \frac{k}{\omega} e^{-\frac{1}{2}} \sqrt{2}$. The geometric and lateral forces of this shape are defined by:

$$y_4(x) = y_1(x) + y_B(x) \quad \forall x \in \left(c - \frac{T}{2}, c + \frac{T}{2}\right) \quad (7)$$

$$F_{x4} = F_{x1} + F_B \quad \forall x \in \left(c - \frac{T}{2}, c + \frac{T}{2}\right) \quad (8)$$

If $y_1(x) = 0$ then $y_4(x) = F_{x4} = 0$. The geometric and lateral components forces of the small saw tooth bump are $y_B(x)$ and F_B respectively, which are defined as follow:

$$\begin{cases} \text{If } x < c \\ y_B(x) = \frac{k}{\omega} e^{-\frac{1}{2}} \sqrt{2} (x-c) + k \\ F_B = -\frac{k}{\omega} e^{-\frac{1}{2}} \sqrt{2} \\ \forall x \in \left(c - \frac{T}{2}, c\right) \end{cases} \quad \begin{cases} \text{If } x \geq c \\ y_B(x) = -\frac{k}{\omega} e^{-\frac{1}{2}} \sqrt{2} (x-c) + k \\ F_B = \frac{k}{\omega} e^{-\frac{1}{2}} \sqrt{2} \\ \forall x \in \left(c, c + \frac{T}{2}\right) \end{cases} \quad (9) \quad (10)$$

In both cases: $k=0.00285$ m, if $y_B(x) \leq 0$ then $F_B = y_B(x) = 0$.

C.5 Sinusoidal segment plus small Gaussian bump ("SineGauss", Fig. 5, case E).

The sinusoidal component is SineSeg. The small Gaussian bump is generated by geometrical and lateral forces with $k=0.00285$ m.

$$y_5(x) = y_1(x) + e^{-\left(\frac{x-c}{\omega}\right)^2} \quad \forall x \in \left(c - \frac{T}{2}, c + \frac{T}{2}\right) \quad (11)$$

$$F_{x5} = F_{x1} + \frac{2k}{\omega^2} (x-c) e^{-\left(\frac{x-c}{\omega}\right)^2} \quad \forall x \in \left(c - \frac{T}{2}, c + \frac{T}{2}\right) \quad (12)$$

If $y_1(x) = 0$ then $y_5(x) = F_{x5} = 0$.

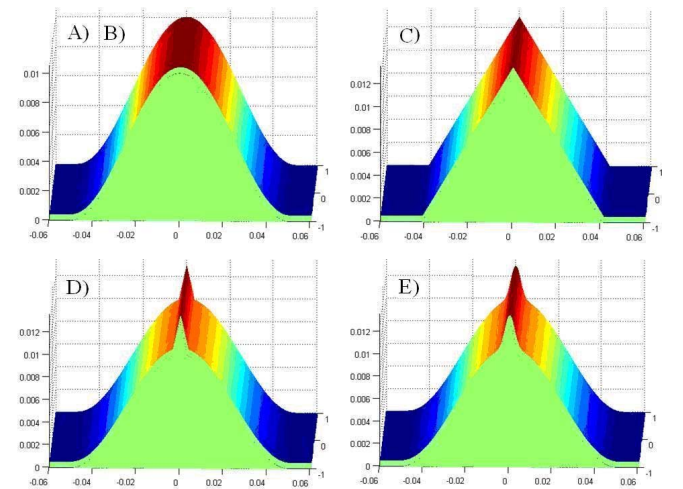


Fig. 5. Sample haptic virtual surfaces, here centered at $c = 0$ m.

III. RESULTS

Table 1 shows subject performance in the haptics-to-vision matching task. This table shows the frequency with which a given haptic surface was matched to one of the visual profiles shown in Fig. 3. This frequency is expressed as a percent of the overall matching performance for all subjects.

Subjects consistently matched the haptic surface SineSeg to the sinusoidal shape (Row 1, Column 1). However, subjects' matching performance was completely different when exploring SineLFGauss (Row 2, Column 2). Note how SineSeg and SineLFGauss had the same geometry.

It is striking how the Saw haptic surface was very frequently matched to the sinusoidal shape segment (Row 3, Column 1). But the converse was not true: the haptic sinusoidal segment (SineSeg) was rarely matched to the sawtooth segment (Row 1, Column 4). This helps highlight the difficulties of consistently rendering a good sawtooth shape by using a literal approach. Even though the stimulus had an approximation to a real, sharp edge, the results suggest that subjects did not perceive an object with a sharp feature.

This contrasts with subjects' matching performance for SineLFGauss (Row 2). This haptic surface was rarely confused with the sinusoid. It was sometimes classified into different categories by some subjects, but overall it was mostly matched to the sinusoidal surface with a small Gaussian bump (Fig. 3, Profile 2) and to the sinusoidal surface with a small sawtooth bump (Fig. 3, Profile 3). This suggests that SineLFGauss was perceived by subjects as a sinusoidal segment with a sharp feature (Fig. 3, Profiles 2 and 3), rather than as a large sawtooth shape (such as the one in Fig. 3, Profile 4).

TABLE I

Haptic Shapes	Matched Visual Shape (%, all subjects)			
	1.Sinusoidal (Fig 2.1)	2.Sinusoidal and small Gaussian (Fig 2.2)	3.Sinusoidal and small sawtooth (Fig 2.3)	4.Sawtooth (Fig 2.4)
1.SineSeg (Fig. 4.A)	96.7	2.2	0.0	1.1
2.SineLFGauss	6.1	28.9	48.9	16.1
3.Saw (Fig. 4.B)	45.6	14.4	3.3	36.7
4.SineSaw (Fig. 4.C)	4.4	16.7	68.9	10.0
5.SineGauss (Fig. 4.D)	6.1	60.0	9.4	24.5

Average Haptic to Visual matching for all subjects. The highlighted cells indicate the visual shapes to which the haptic shapes should be ideally matched. For each haptic shape, the difference in matching performance is statistically significant (ANOVA, $p < 0.01$)

In contrast to the matching performance for the haptic Saw (Table 1 row 3), haptic surfaces SineSaw and SineGauss were rarely matched (4.4 % and 6.1 % respectively) to the visual sinusoidal segment (Column 1, rows 4 and 5). This suggests that the perception of sharp

features depends on the context in which they are presented. For example, when exploring haptic shapes SineLFGauss, SineSaw and SineGauss, there was a decrease in force as the top of the sinusoidal position of the stimuli was reached, and then the sharp feature or the Gaussian lateral force provided a large increase in force. Compare this to the constant forces experienced when ascending/descending the slopes of Saw (see "Haptic Shapes" in Methods). This may not be surprising from the perceptual point of view, but it is potentially useful for haptic rendering purposes. Finally, subjects consistently matched SineSaw and SineGauss to the equivalent visual shapes: 68.9 % and 60 % of the time, respectively.

Subjects' finger trajectories during object exploration were compared to the ideal geometries of each haptic surface through Mean Squared Errors (MSEs). This allowed examining how close subjects' finger trajectories were to the geometry of each stimulus. Fig. 6 shows a typical trajectory when exploring a SineSaw stimulus. Subjects' finger trajectories had a slight vertical offset relative to the ideal geometry of the objects. This was due to the finite stiffness used (which in this experiment was set to 2 N/mm). The offset was eliminated before computing MSEs. MSEs were calculated within the range $x \in (c - 0.025m, c + 0.025m)$.

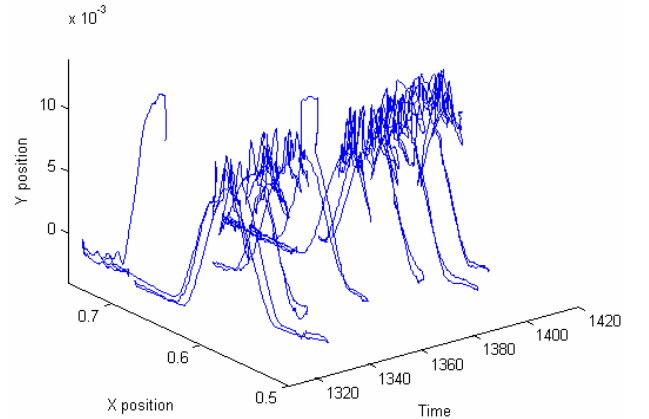


Fig. 6. An user's fingertip trajectory while exploring a SineSaw shape (Subject 1, trial 34).

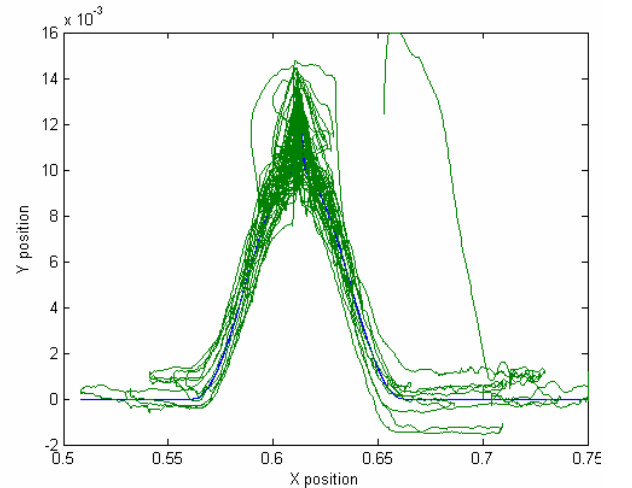


Fig. 7. Trajectory data corrected for vertical offset and ready for MSE computation.

MSE analysis is summarized in Table 2. Results are expressed as a percent of the trials in which a given trajectory was closest to the geometry of a haptic shape. For example, consider all the trials in which SineSeg was explored by subjects (Table 2, row 1). Table 2 shows that in 98.33% of those trials, subjects' finger trajectories were closest to the ideal SineSeg geometry. The table also indicates that, very rarely, subjects' finger trajectories were closest to the ideal geometries of Saw, SineSaw or SineGauss.

TABLE II

Haptic Shape explored	Closest geometry match of exploration trajectory (percent of total trials for each haptic shape)			
	1.SineSeg	2.Saw	3.SineSaw	4.SineGauss
1. SineSeg (Fig. 4.A)	98.33	0.56	0.56	0.56
2. SineLFGauss	91.67	1.67	4.44	2.22
3. Saw (Fig. 4.B)	1.11	92.78	1.11	5.00
4. SineSaw (Fig. 4.C)	15.00	26.67	56.11	2.22
5. SineGauss (Fig. 4.D)	2.22	36.67	21.11	40.00

Comparison of the exploration trajectories used by subjects to the geometry of the haptic shapes. Note that SineLFGauss stimuli had the same geometry as the Sinusoidal segment (SineSeg). For each haptic shape, the difference in the trajectories followed is statistically significant (ANOVA, $p < 0.01$).

Table 2 helps assess the difficulty to render the geometry of some sharp features. While rendering the geometry of SineSeg and Saw was simple, this was not the case for SineSaw and SineGauss (rows 4 and 5). Subjects' finger trajectory when exploring SineSaw and SineGauss did not, in general, closely follow the target geometry of these surfaces. In contrast, rendering the geometry of SineLFGauss was possible (row 2). As mentioned above, SineLFGauss had the same geometry as SineSeg (a smooth sinusoid), but was consistently matched to visual shapes with sharp features. The difficulties to render the geometry of SineSaw and SineGauss suggest that maintaining surface contact with these objects during exploration was made difficult by the surfaces' sharp features, which is something commonly observed when rendering these in general. In contrast, Table 2 suggests that good surface contact with SineLFGauss (the surface with an illusory Gaussian bump) was simply achieved.

Two major points are suggested by Table 2 also. The first is that the geometry of Saw was accurately rendered (Table 2, Row 3, Column 2), but this did not result in subjects consistently matching this haptic surface to the visual Sawtooth profile (Table 1, Row 3, Column 4). In contrast, the haptic Saw was consistently matched to the sinusoidal visual profile (Table 1, Row 3, Column 1). This suggests that accurate rendering of the geometry of sharp objects does not always result in subjects perceiving the sharp features of objects.

The second major point is that, even when the geometry is not very accurately rendered (perhaps due to unstable contact with the surface of the object due to spatially sharp features), subjects still could be able to perform an accurate

haptic to visual match. This is suggested by the matching performance for SineSaw (Table 1, Row 4, Column 3).

IV. DISCUSSION AND FUTURE WORK

The results suggest that lateral-force-based haptic shape illusions (such as the one used in SineLFGauss) can be combined with a smooth object geometry to haptically render sharp features of objects. The results also suggest that this can be achieved while maintaining a stable contact with the object, which is what happens, in general, during haptic interaction with real objects with spatially sharp features. It is not possible to stress enough the desirability of such stable interaction with haptically rendered, spatially sharp objects, particularly in applications such as surgery simulators. However, the variability found during haptic to visual matching for SineLFGauss suggests that there are more factors determining subject perception in these cases. For example, subjects may have had a bias toward choosing one of the three visual figures, or perhaps subjects' expectations regarding the haptic features of stimuli were modulated by the visual shapes. More research is needed to clarify these possibilities.

Nevertheless, the data suggest that the approach is promising, and that perceptual illusions may help overcome some intrinsic limitations of haptic rendering methods due to inertial properties of limbs and mechanical limitations of interfaces, for example. The use of haptic illusions, in particular lateral-force-based ones, suggests a variety of other, different methods to render sharp features. One of these methods is schematically described in Fig. 8. Here, an object with a smooth geometry (a rectangle with smooth corners), is combined with two illusory, lateral-force-based "holes" [5,6] (represented in Fig. 8 by two ellipsoidal segments). The net result could be, perceptually, a very sharp corner, schematically depicted in Fig. 8 by the curve formed by the two ellipsoidal segments. However, as happened with SineLFGauss in our experiment, a user's spatial trajectory when exploring such an object would be smooth (along the square in Fig. 8), to help ensure contact stability.

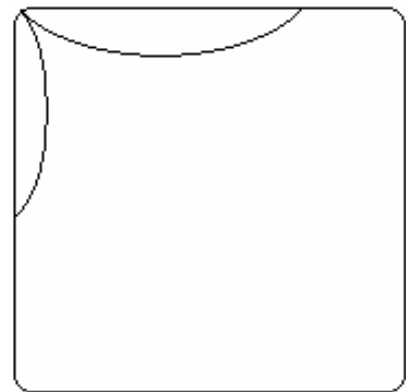


Fig. 8. An alternative haptic rendering method for sharp corners: two illusory "holes" (ellipsoidal segments) are used to perceptually create a very sharp corner (top left corner of the square) when exploring an object with smooth geometry (square). See text for details.

REFERENCES

- [1] Basdogan, C. and M. A. Srinivasan (2002). Haptic Rendering in Virtual Environments. Handbook of Virtual Environments. K. Stanney. London, Lawrence Earlbaum, Inc.: Chapter 6, pp. 117-134.
- [2] Hayward, V., Astley, O. R., Cruz-Hernandez, M., Grant, D. Robles-De-La-Torre, G. Haptic Interfaces and Devices. Sensor Review 24(1):16-29 (2004).
- [3] Minsky, M (1995) Computational Haptics: The Sandpaper System for Synthesizing texture for a force-feedback display. Ph.D. dissertation, Massachusetts Institute of Technology.
- [4] Morgenbesser, H.B., & Srinivasan, M.A. (1996). Force shading for haptic shape perception. Proceedings of the ASME Dynamic Systems and Control Division, DSC-Vol. 58, 407-412.
- [5] Robles-De-La-Torre, G. & Hayward, V. (2000). Virtual Surfaces and Haptic Shape Perception. Proceedings of the Haptic Interfaces for Virtual Environment and Teleoperator Systems Symposium, ASME International Mechanical Engineering Congress & Exposition 2000, Orlando, Florida, USA.
- [6] Robles-De-La-Torre, G. & Hayward, V. (2001). Force Can Overcome Object Geometry In the perception of Shape Through Active Touch. Nature 412 (6845):445-8.
- [7] Ho PP, Adelstein BD, Kazerooni H (2004). Judging 2D versus 3D Square-Wave Virtual Gratings. Proceedings of the 12th International Symposium on Haptic Interfaces for Virtual Environment and Teleoperator Systems (HAPTICS'04) pp. 176-183.
- [8] Avizzano, C.A.; Marcheschi, S.; Angerilli, M.; Fontana, M.; Bergamasco, M.; Gutierrez, T.; Mannegeis, M. (2003). A multi-finger haptic interface for visually impaired people. Proceedings of the 12th IEEE International Workshop on Robot and Human Interactive Communication. 31 Oct.-2 Nov. 2003 Page(s):165 - 170 .
- [9] Avizzano C.A., Marcheschi S., Bergamasco M. Haptic Interfaces: Collocation and Coherence Issues (2004). In Proc. of Multi-point Interaction in Robotics and Virtual Reality Workshop, IEEE International Conference in Robotics and Automation.
- [10] Iglesias, R.; Casado, S.; Gutierrez, T.; Barbero, J.I.; Avizzano, C.A.; Marcheschi, S.; Bergamasco, M. (2004). Computer graphics access for blind people through a haptic and audio virtual environment. Proceedings of the 3rd IEEE International Workshop on Haptic, Audio and Visual Environments and Their Applications.